Negative index of refraction in optical metamaterials

Vladimir M. Shalaev, Wenshan Cai, Uday K. Chettiar, Hsiao-Kuan Yuan, Andrey K. Sarychev, Vladimir P. Drachev, and Alexander V. Kildishev

School of Electrical and Computer Engineering, Purdue University, West Lafayette, Indiana 47907

Received September 13, 2005; accepted October 14, 2005

A double-periodic array of pairs of parallel gold nanorods is shown to have a negative refractive index in the optical range. Such behavior results from the plasmon resonance in the pairs of nanorods for both the electric and the magnetic components of light. The refractive index is retrieved from direct phase and amplitude measurements for transmission and reflection, which are all in excellent agreement with simulations. Both experiments and simulations demonstrate that a negative refractive index $n' \approx -0.3$ is achieved at the optical communication wavelength of 1.5 μm using the array of nanorods. The retrieved refractive index critically depends on the phase of the transmitted wave, which emphasizes the importance of phase measurements in finding n'. © 2005 Optical Society of America

OCIS codes: 160.4670, 260.5740, 310.6860.

One of the most fundamental notions in optics is that of the refractive index, which gives the factor by which the phase velocity of light is decreased in a material compared with vacuum conditions. In materials with a negative refractive index the phase velocity is directed against the flow of energy. There are no known naturally occurring negative-index materials (NIMs). Proof-of-principle experiments[1] have shown that artificially designed materials (metamaterials) can act as NIMs at microwave wavelengths. NIMs drew a large amount of attention after Pendry predicted that NIMs can act as a superlens allowing imaging resolution that is limited not by the wavelength but rather by material quality.[2] The near-field version of the superlens has already been reported.[3,4] Materials that can be characterized by a dielectric permittivity $\epsilon = \epsilon' + i\epsilon''$ and a magnetic permeability $\mu = \mu' + i\mu''$ have a negative real part of the complex refractive index if the sufficient (but not necessary) conditions $\epsilon' < 0$ and $\mu' < 0$ are fulfilled.[5]

Recent experiments showed that a magnetic response and a negative permeability can be obtained in the terahertz spectral ranges.[6–8] However, the ultimate goal, a negative refractive index, was not achieved in those experiments. In parallel with progress for metal–dielectric metamaterials, two experimental demonstrations of negative refraction in the near IR range have been made in GaAs-based photonic crystals[9] and in Si-polyimide photonic crystals.[10]

Below we report our experimental demonstration of a negative refractive index material for the optical range, specifically for wavelengths close to 1.5 μm (200 THz frequency), accomplished with a metal–dielectric composite. The NIM structural design used follows our theoretical prediction of negative refraction in a layer of pairs of parallel metal nanorods.[11,12]

For normally incident light with the electric field polarized along the rods and the magnetic field perpendicular to the pair [Fig. 1(a)], the electric and magnetic responses both can experience resonant behavior at certain frequencies. Above the resonance frequency, the circular current in the pair of rods can lead to a magnetic field opposing the external magnetic field of the light. The excitation of plasmon resonances for both the electric and the magnetic light components results in the resonant behavior of the refractive index, which can become negative above the resonance as previously predicted.[11,12] This resonance can be thought of as a resonance in an optical LC circuit, with the metal rods providing the inductance L and the dielectric gaps between the rods acting as capacitive elements C. Note that coupling between metal rods may lead to other interesting optical properties.[13]

We performed our experiments with a 2 mm $\times$ 2 mm array of nanorods on a glass substrate fabricated using electron-beam lithography with a JEOL JBX-6000FS writer. To prevent a charging effect in the case of the glass substrate, a thin Cr layer was deposited on top of the double layer of poly(methyl-

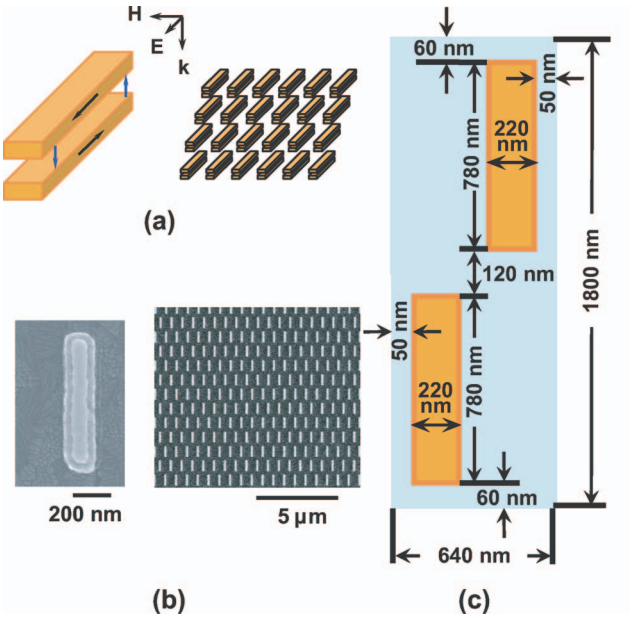

Fig. 1. (a) Schematic for the array of nanorod pairs. (b) Field-emission scanning electron microscope images. (c) Elementary cell.

0146-9592/05/243356-3/$15.00

methacrylate) photoresist. Then, after writing, the Cr layer was removed with appropriate etching. The desired sandwich structure, Ti(5 nm)/Au (50 nm)/Ti(5 nm)/SiO_2(50 nm)/Ti(5 nm)/Au(50 nm), was deposited serially in an electron-beam vacuum evaporator. The fabrication procedure resulted in a trapezoidal shape of the rods. Figure 1(b) shows field-emission scanning electron microscope images of a portion of the sample and a closer view of a single pair of rods. The dimensions of the bottom rods (780 nm$\times$220 nm) and the elementary cell are shown in Fig. 1(c). The top rods are smaller (670 nm$\times$120 nm). The metal filling factor is 13.5%.

In our simulation based on a 3D finite-difference time domain (FDTD) method,[14] the overall geometry of the nanorods followed the trapezoidal shape of the actual sample. To simulate the permittivity of gold, the Drude model $\epsilon_{Au}=9.0-(1.3673\times10^{16})^2/[\omega^2+i(1.0027\times10^{14})\omega]$, where $\omega=2\pi c/\lambda$, was transformed into a matching Debye model. The Debye model provides excellent agreement with the measured optical constants in the spectral range of interest. The elementary cell with $x\times y\times z=1.8\ \mu$m $\times0.64\ \mu$m$\times4\ \mu$m was illuminated by a monochromatic plane wave at normal incidence. Since we used a uniform grid with a spatial resolution of 10 nm, the 5 nm Ti layers were not taken into account. The thick glass layer was considered infinite in the simulations. The reflected and transmitted electric fields, E_r and E_t, are calculated for the layer of the nanorods with normally incident field E_i. Then, $r=\alpha E_r(-d)/E_i(-d)$ and $t=\alpha E_t(d)/E_i(-d)$ are obtained, where $\alpha=\exp[ik(\Delta-2d)]$, k is the wavenumber in air, $\Delta=160$ nm, and d is the distance from the center of the layer to the evaluation planes in front and behind the sample. The distance d is chosen so that the reflected and transmitted waves (E_r and E_t) are plane waves with less than 1% deviation in magnitudes in the evaluation planes.

The complex index of refraction ($n=n'+in''$) of the nanorod layer on a substrate is found from

$$\cos nk\Delta=\frac{1-r^2+n_st^2}{(n_s+1)t+rt(n_s-1)},\qquad(1)$$

where n_s is the refractive index of the substrate ($n_s=1.48$ for our glass substrate). Specifically, we obtain the impedance $Z=Z'+iZ''$ (not shown here) and the refractive index of the equivalent homogeneous layer with the same complex reflectance r and transmittance t as the actual array of nanorods. Equation (1) gives the refractive index of a thin layer of a passive material ($n''>0$ and $Z'>0$). Note that for a thin layer such retrieval can be performed unambiguously.[15] Since a linear polarization of light is preserved under propagation through our anisotropic sample, when the polarization is parallel to the main axes, we solve Eq. (1) independently for light polarized parallel and perpendicular to the nanorods.

The amplitudes and phases for transmittance and reflectance needed for retrieval of the refractive index were measured directly in our experiments. The transmission ($T=|t|^2$) and reflection ($R=|r|^2$) spectra are measured with a Lambda 950 spectrophotometer from Perkin-Elmer using linearly polarized light. The transmission spectra are collected at normal incidence, and the reflection spectra are measured at a small incident angle of 8°. Control measurements of the reflectance performed with a laser source at 0.5° of the incident angle show no significant difference.

The phase measurements were performed with polarization and walk-off interferometers using tunable diode lasers. In the polarization interferometer, two optical channels have a common geometrical path and differ by the polarization of light. This allows one to measure the phase difference between orthogonally polarized waves $\Delta\phi=\phi_\parallel-\phi_\perp$ caused by anisotropy of a refractive material. The walk-off interferometer has two optical channels that differ in geometrical paths; this gives a phase shift introduced by a sample (ϕ_s) relative to a reference layer of air with the same thickness (ϕ_r): $\delta\phi=\phi_s-\phi_r$. The walk-off effect in calcite crystals is employed to separate the two beams and then bring them together to produce interference. The instrumental error of the phase anisotropy measurement by polarization interferometer is ±1.7°. We note that variations in the substrate thickness do not affect the results of our phase anisotropy measurements, which is typical for common path interferometers. In the case of the walk-off interferometer, the thickness variation gives an additional source of error, causing the error for the absolute phase shift measurements to increase up to ±4°. A more detailed description of our phase mea-

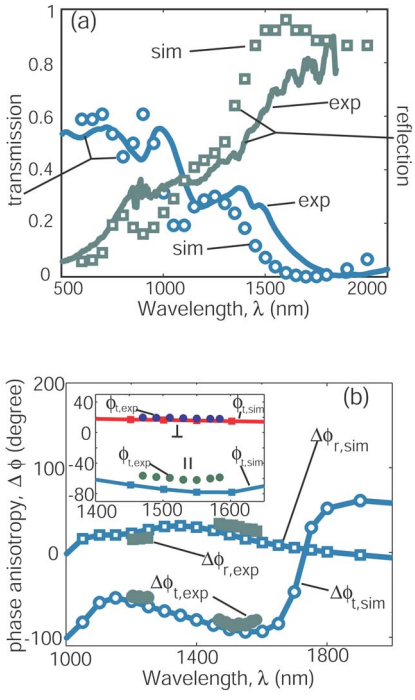

Fig. 2. (Color online) (a) Reflection and transmission spectra: experiments (solid curves) and simulations (squares and circles). (b) Phase anisotropy $\Delta\varphi$ for reflection (squares) and transmission (circles), from experiments and simulations. Inset, absolute phase shifts $\delta\varphi$ in transmission for the parallel (lower) and perpendicular (upper) polarizations of light.

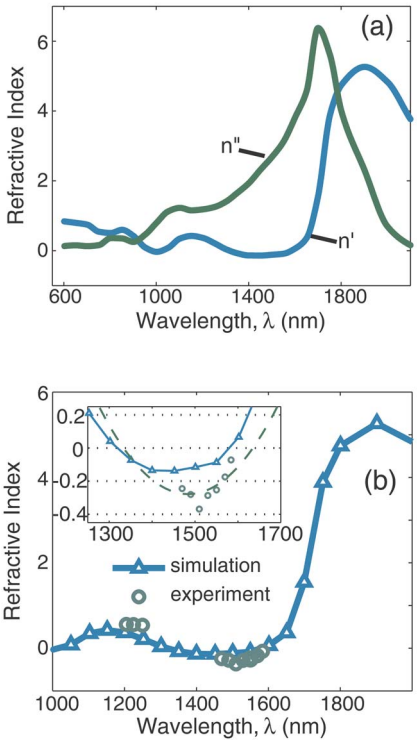

Fig. 3. (Color online) (a) Real and imaginary parts of the refractive index retrieved from simulations. (b) Real part of the refractive index retrieved from simulations (triangles) and experiments (circles). The inset in (b) is a magnified view of the region of negative refraction; the dashed curve shows the quadratic least-squares fit for the experimental data.

surements will be published elsewhere. We note here that the linear polarization of light is well preserved after propagation through the sample for both light polarizations, parallel and perpendicular to the rods. Specifically, the light ellipticity (the intensity ratio for the two components) changes only from 10^{-3} to 3×10^{-3}. Thus the method used provides direct measurements of the magnitude and sign of the phase shift for the two linearly polarized components of light.

Figure 2 shows results of our measurements of amplitudes and phases for transmitted and reflected waves. The system of parallel gold nanorods shows a strong plasmonic resonance near 1.5 μm for both amplitude [Fig. 2(a)] and phase shift [Fig. 2(b)] of light with the electric field polarized parallel to the rods. For the electric field polarized perpendicular to the rods the spectral dependences are rather flat from 1 to 2 μm, and the plasmon resonance occurs near 800 nm (not shown). We note good agreement between our 3D FDTD simulations and experimental data.

Figure 3 shows the retrieved refractive index and demonstrates excellent agreement between measurements and simulations [Fig. 3(b)]. The obtained phase shift of −61° in the light transmittance at $\lambda=1.5$ μm is well below the phase shift in air $-\phi_0=-40°$ at 1.5 μm; thus the negative phase acquired in the sample is ≈−21°. The refractive index is negative between 1.3 and 1.6 μm, with $n'=-0.3\pm0.1$ at $\lambda=1.5$ μm. Note a rather high transmittance of ≈25% and relatively low absorption of ≈10%. The imaginary part of the refractive index also shows resonant behavior and it is large near the resonance. Our calculations show that by optimizing the system (e.g., by matching impedances), the ratio of the real and imaginary parts of the refractive index can be significantly increased.

In conclusion, for an array of pairs of parallel gold rods, we obtained a negative refractive index of $n'\approx-0.3$ at the optical communication wavelength of 1.5 μm. This new class of negative-index materials is relatively easy to fabricate on the nanoscale and opens new opportunities for designing negative refraction in optics.

This work was supported in part by NSF-NIRT award ECS-0210445 and by ARO grant W911NF-04-1-0350. V. M. Shalaev's e-mail address is shalaev@purdue.edu.

References

1. R. A. Shelby, D. R. Smith, and S. Schultz, Science **292**, 77 (2001).
2. J. B. Pendry, Phys. Rev. Lett. **85**, 3966 (2000).
3. N. Fang, H. Lee, and X. Zhang, Science **308**, 534 (2005).
4. D. O. S. Melville and R J. Blaikie, Opt. Express **13**, 2127 (2005).
5. V. G. Veselago, Sov. Phys. Usp. **10**, 509 (1968) [Usp. Fiz. Nauk **92**, 517 (1964)].
6. T. J. Yen, W. J. Padilla, N. Fang, D. C. Vier, D. R. Smith, J. B. Pendry, D. N. Basov, and X. Zhang, Science **303**, 1494 (2004).
7. S. Linden, C. Enkrich, M. Wegener, J. Zhou, T. Koschny, and C. Soukoulis, Science **306**, 1351 (2004).
8. S. Zhang, W. Fan, B. K. Minhas, A. Frauenglass, K. J. Malloy, and S. R. J. Brueck, Phys. Rev. Lett. **94**, 037402 (2005).
9. A. Berrier, M. Mulot, M. Swillo, M. Qiu, L. Thylén, A. Talneau, and S. Anand, Phys. Rev. Lett. **93**, 073902 (2004).
10. E. Schonbrun, M. Tinker, W. Park, and J.-B. Lee, IEEE Photon. Technol. Lett. **17**, 1196 (2005).
11. V. A. Podolskiy, A. K. Sarychev, and V. M. Shalaev, J. Nonlinear Opt. Phys. Mater. **11**, 65 (2002).
12. V. A. Podolskiy, A. K. Sarychev, and V. M. Shalaev, Opt. Express **11**, 735 (2003).
13. Y. Svirko, N. Zheludev, and M. Osipov, Appl. Phys. Lett. **78**, 498 (2001).
14. A. Taflove and S. Hagness, *Computational Electrodynamics: the Finite-Difference Time-Domain Method* (Artech, 2000).
15. D. R. Smith, S. Schultz, P. Markôs, and C. M. Soukoulis, Phys. Rev. B **65**, 195104 (2002).